ARMY RESEARCH LABORATORY

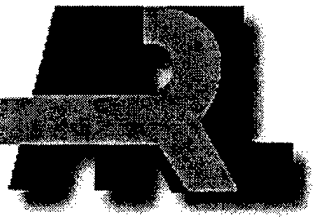

Interior Ballistic Simulations of the Bulk-Loaded Liquid Propellant Gun

James DeSpirito

ARL-TR-2316 JANUARY 2001

The findings in this report are not to be construed as an official Department of the Army position unless so designated by other authorized documents.

Citation of manufacturer's or trade names does not constitute an official endorsement or approval of the use thereof.

Destroy this report when it is no longer needed. Do not return it to the originator.

ERRATA SHEET

RE: ARL-TR-2316, "Interior Ballistic Simulations of the Bulk-Loaded Liquid Propellant Gun," by James DeSpirito of the Weapons & Materials Research Directorate, U.S. Army Research Laboratory

The last line of page 15 is repeated at the top of page 16.

Army Research Laboratory
Aberdeen Proving Ground, MD 21005-5066

ARL-TR-2316 January 2001

Interior Ballistic Simulations of the Bulk-Loaded Liquid Propellant Gun

James DeSpirito
Weapons & Materials Research Directorate

Abstract

The objective of this study was to determine the feasibility of modeling the interior ballistic processes of the bulk-loaded liquid propellant gun. A modified version of the CRAFT[1] Navier-Stokes code was used to perform simulations of bulk-loaded liquid propellant gun firings that employed two different chamber configurations. The simulation accurately captures the longitudinal wave structure present in the experimental data, but a combustion delay present at the start of the ballistic cycle was not present in the simulations. The simulations showed the development of a cavity that penetrated the bulk-liquid column as it accelerated toward the projectile, leaving an annulus of unburned liquid propellant along the chamber wall. High gas temperatures were noted in this gas cavity region, possibly attributable to isentropic compression caused by the unique conditions in the bulk-loaded gun. The simulation of the second chamber configuration compared well with the experimental data, while the simulation of the first chamber configuration did not capture the experimental pressure-time profile. In general, the simulations showed an insensitivity to chamber geometry that is not observed in experimental firings. The limitations of the simulations were attributed to the lack of complete physical sub-models, such as a droplet formation/combustion model and detailed chemical kinetics. The model has the potential to be a useful tool in the analysis of experimental data. However, predictive capability is unlikely without the development of better physical sub-models.

[1] not an acronym

ACKNOWLEDGMENTS

The author would like to thank Michael Nusca and Todd Rosenberger of the U.S. Army Research Laboratory for reviewing the manuscript; Ashvin Hosangadi of Combustion Research and Flow Technology, Inc., for modifications of the CRAFT code and for his help and many useful discussions during this effort; and Robert Talley and John Owczarczak of Veritay Technology, Inc., for supplying the experimental data used during this study.

This work was supported in part by a grant of high performance computing time from the Department of Defense High Performance Computing Center at Aberdeen Proving Ground, Maryland.

INTENTIONALLY LEFT BLANK

Contents

Figures

INTERIOR BALLISTIC SIMULATIONS OF THE BULK-LOADED LIQUID PROPELLANT GUN

1. Introduction

The use of liquid propellant (LP) in guns has been the focus of recurrent research efforts for nearly 50 years (Morrison, Knapton, & Bulman 1988; Klingenberg, Knapton, Morrison, & Wren 1997). The interior ballistic processes in liquid propellant guns are much different from those in conventional solid propellant guns. In conventional guns, the interior ballistics are controlled by the combustion of solid propellant grains, which are manufactured with a predetermined propellant formulation and grain geometry. The propellant formulation and the grain geometry control the gas generation rate by affecting the linear burning rate and the total burning surface area of the grain, respectively. In contrast, the interior ballistics of the liquid propellant gun are determined by either the rate of injection of LP into the combustion chamber, as in the regenerative liquid propellant gun, or the hydrodynamics of the combustion gas-liquid propellant mixing process, as in the bulk-loaded liquid propellant gun (BLPG). In the regenerative liquid propellant gun, the surface area required to burn the propellant is determined by the break-up of the liquid jet as it enters the combustion chamber. In the BLPG, the propellant surface area is generated by the break-up of the gas-liquid interface separating the bulk liquid and the gaseous combustion products.

The primary focus of LP-related research over the past 15 years was on the regenerative liquid propellant gun, which was shown to offer control and repeatability of the ballistic cycle (Morrison, Knapton, & Bulman, 1988; Klingenberg, Knapton, Morrison, & Wren 1997). The last large caliber research program to develop a BLPG ended in the 1970's after several catastrophic failures. Research interest in the BLPG was revived in the early 1990's (Talley & Owczarczak 1991, 1994; Rosenberger, Stobie, Knapton, 1995a, 1995b; Talley, Owczarczak, & Geise 1997). The concept is attractive because it is less complex than the regenerative liquid propellant gun and offers some advantages for small and medium caliber direct fire weapons. However, the interior ballistic process in the BLPG is not as well understood and the modeling tools are not as advanced as they are for the regenerative liquid propellant gun.

Several interior ballistic models were developed during the height of the BLPG work in the 1970's. These ranged in complexity from simple, zero-dimensional (0-D) (Edelman 1974; Burnett 1976) and one-dimensional (1-D) models (Edelman 1976) to two-dimensional (2-D), axisymmetric solutions of the Navier-Stokes equations (Edelman, Phillips, & Wang 1983). The 0-D and 1-D models required empirical information and were based on the phenomenological model

of Comer, Shearer, and Jones (1963). This phenomenological model, which was proposed to be consistent with the physical situation and the experimental data, is illustrated in Figure 1 and is presented as follows. First, the ignition process creates a bubble or cavity of hot combustion products at the axial position of the breech (rear) end of the gun. Such a gas cavity can be generated by venting hot gases from an external igniter directly into the fluid in the combustion chamber. The ignition process causes the development of pressure waves, predominantly longitudinal. These pressure waves are believed to cause the gas-liquid interface at the cavity to spall, increasing the rate of mixing of propellant and hot combustion products. After the projectile begins to move, the high-pressure gases in the cavity accelerate both the projectile and the "slug" (i.e., column or volume) of LP between the projectile and cavity. This situation is similar to the hydrodynamic instability of accelerated liquid surfaces analyzed by Taylor (1950). The growth of this instability leads to the development of a "Taylor" cavity, which penetrates the liquid column until it reaches the projectile. After the cavity reaches the projectile base, an annulus of liquid is believed to remain on the chamber wall, with combustion gases flowing through the center. This leads to the Kelvin-Helmholtz type instability at the gas-liquid interface, with an increased combustion rate attributable to enhanced turbulent mixing. This phenomenological model can be used to explain many of the phenomena observed in experimental BLPG data. However, another mechanism may be responsible for achieving the very high burning rates necessary to explain some of the experimental data, especially when anomalies occur. Pressure-time traces qualitatively similar to experimental results were produced with these early 0-D and 1-D models, and some insight was gained from the results. Although some of these models were used with some success in analyzing experimental data, they had little predictive capability.

The 2-D axisymmetric model of Edelman, Phillips, and Wang (1983) was an attempt to model the hydrodynamic and chemical processes present in the BLPG. The model included the framework to treat the processes in the BLPG: turbulence (algebraic and two-equation models), droplet formation, and finite rate chemical kinetics. With a simplified, one-step combustion mechanism, a favorable comparison between predictions of chamber pressure and experimental data was shown. The development of the Taylor cavity was also observed in the simulation. Development of this model for this application apparently ended with the conclusion of BLPG research in the late 1970's.

Another model to describe the interior ballistics of the BLPG was proposed by Kuo, Cheung, and Chen (1989). This was another 2-D axisymmetric formulation that also included mechanisms of droplet dispersion and Helmholtz instability to estimate the liquid entrainment rate and droplet distribution. Numerical calculations were not reported, but the methods presented were later used in a model of the liquid propellant electro-thermal-chemical (LPETC) gun (Chen, Kuo, & Cheung 1992) that compared well with experimental data.

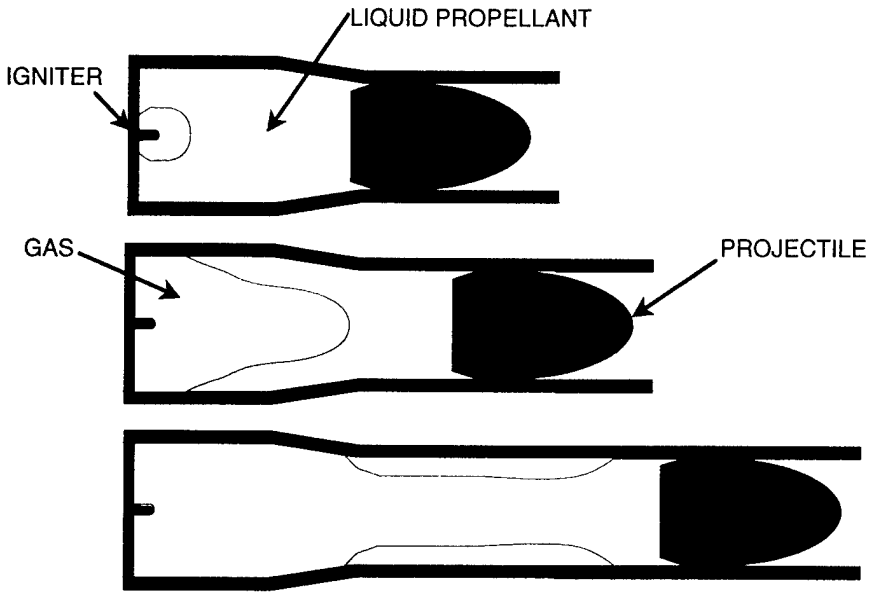

Figure 1. Phenomenological Model of the BLPG Interior Ballistics Proposed by Comer, Shearer, and Jones (1963).

A more recent model by Macpherson, Bracuti, and Chiu (1994) was based on the BLPG operating in supercritical conditions. Rather than follow the traditional model of Comer, Shearer, and Jones (1963), they assumed that the LP was supercritical throughout the process, and they included heat transfer in the fluid as well as chemical kinetics. The combustion results from a thermal wave moving through the fluid, starting from an initial hemispherical "ignition bubble" that was specified as a boundary condition. The model compared reasonably to a specific set of experimental data used to calibrate the model.

The issue of supercritical conditions was also considered by Edelman, Phillips, and Wang (1983), who suggested the possibility that a gas-gas (i.e., combustion gas-supercritical "fluid") type mixing might be applicable. Most, if not all, earlier BLPG models considered gas-liquid interactions.

The experience gained in developing the 2-D BLPG model was later used to model the LPETC gun (Hsiao, Phillips, & Su, 1992), which is similar to the BLPG. In the LPETC gun, the combustion of a liquid propellant is initiated and (potentially) controlled by the injection of a plasma generated from the discharge of electrical energy. In the BLPG, the liquid propellant is only initiated by the injection of hot gas from an igniter. Several other 2-D models of the LPETC gun were also developed (Cook, Dyvik, & Chryssomallis 1989; Chen, Kuo, & Cheung 1992; Hosangadi, Sinha, & Dash 1995). Results from these models compared quite well to specific experimental data.

The sensitivity of various BLPG design parameters, such as igniter location, igniter output, and boundary conditions, has been largely unexplored because a validated, predictive computer model does not exist. This is primarily because of the difficulty in identifying, through diagnostic experimentation, the physical processes that occur at gun pressures as great as 700 MPa. Many of these difficulties remain. However, the codes developed for the LPETC gun also contain the framework for simulating the combustion processes in the BLPG and provide a good starting point for developing a model of the BLPG.

For this study, the CRAFT[1] Navier-Stokes code (Sinha, Dash, & Hosangadi 1992) was used to model two BLPG concepts that were also investigated experimentally. The goal of this study was to evaluate the effectiveness of using state-of-the-art numerical techniques to model the BLPG process via relatively simple physical models for LP combustion and mixing. If reasonably successful results with these simple models were obtained, then the feasibility of developing more advanced physical models could be estimated. A minimum of two experimental configurations was chosen to determine the sensitivity of the simulation results to changes in combustion chamber geometry. This report describes the results obtained via the CRAFT code to simulate two BLPG concepts and the comparison of those results with experimental data.

2. Numerical Technique

The CRAFT code is based on the TUFF[1] aerodynamic code developed by Molvik and Merkle (1989). It is a 3-D, finite volume code that uses an implicit, upwind scheme based on that of Roe (1981). The total variation-diminishing (TVD) technique of Chakravarthy and Osher (1983) was used to obtain higher order accuracy without spurious oscillatory behavior. A large-eddy simulation (LES) approach was used for turbulence modeling, i.e., the large-scale turbulent structure was directly simulated by the flow solver, while the small-scale (on the order of the grid cell size) dissipative structures were modeled. In the code version used in the present study, a third order accurate TVD scheme, second order time integration, and a simple small-scale (sub-grid) turbulence model were used. A summary of the CRAFT code numerics and modifications for short duration transient, chemically reacting, multi-phase flows was provided by Hosangadi, Sinha, and Dash (1995). They also presented several fundamental numerical validation studies that demonstrate the capability of the CRAFT code to analyze problems involving finite rate combustion, turbulence with large-scale vortical structures and transient wave processes particular to gun propulsion systems. The CRAFT code was successfully used to simulate flows in the electro-thermal-chemical gun and the regenerative liquid propellant gun

[1] not an acronym

(Hosangadi, Sinha, & Dash 1995; Hosangadi, Kenzakowski, Sinha, & Dash 1996; Madabhushi, Hosangadi, Sinha, & Dash 1995), and unsteady jet flow fields (Sinha, Dash, & Madabhushi 1993). All calculations were performed in serial mode on the Silicon Graphics, Inc., Power Challenge Array (SGI-PCA) system at the Department of Defense High Performance Computing Center at Aberdeen Proving Ground, Maryland.

The version of the CRAFT code used for the LPETC gun simulations was modified to perform 2-D axisymmetric simulations of a BLPG. This version of the code uses a mixing length, turbulent eddy viscosity, sub-grid stress model for the finer scales of turbulence. The numerical formulation in the CRAFT code allows for generalized fluid mixtures of gas and bulk liquid. In addition, an equilibrium formulation is used, in which at a given location, the gas and liquid phases have identical velocities, pressures, and temperatures. The combustion model is an Arrhenius-type formulation in which the kinetic rate is based on temperature. The combustion of the bulk liquid propellant, a monopropellant, is modeled as a two-step process. First, the bulk liquid is converted to an intermediate gaseous form (LP vapor). Second, the single, gaseous intermediate species then burns to generate the product species. The numerical values of the rate coefficients are estimated by numerical simulations of earlier liquid propellant closed chamber combustion experiments (DeSpirito 1988); the rate of pressure rise is then matched. These rate coefficients are only estimates and are considered adequate since it is known that this combustion model does not fully describe the combustion process in the BLPG, as discussed in the following paragraphs.

The temperature-based combustion model was chosen for these investigations instead of a pressure-dependent propellant burn rate equation. The latter is used in conventional (solid propellant) interior ballistic analyses and requires knowledge of the propellant burning surface area, which is calculated from the geometry form function. In contrast, in the BLPG, the propellant surface area is generated as a result of the fluid dynamic shear stress between the gas and liquid and is therefore very difficult to calculate. A model of droplet formation, based on shearing at the gas-liquid interface, is required for a pressure-dependent formulation. The temperature-based combustion model should provide acceptable results if the combustion process in the BLPG is dominated by turbulent mixing, i.e., the combustion rate is much faster than the mixing rate. This condition was found in the LPETC gun (Hosangadi, Sinha, & Dash 1995).

The forcing of temperature equilibrium between the gas and the liquid in each cell led to a dependence of the combustion rate on the cell size. Since the temperature of the gas is much greater than that of the liquid, it is believed that the larger cells cause a larger amount of the total liquid to heat at a given time step than would occur on a finer grid. This leads to a faster combustion rate with the large cell size. This problem was noted and new reaction rate coefficients

were estimated by the closed chamber numerical study with a finer grid spacing comparable to that used for the BLPG simulations. A two-temperature formulation appears to be more appropriate and should be implemented into the code in the future.

It was realized at the outset that some aspects of the experimental pressure-time curves would not be captured by this combustion model formulation. For example, the combustion enhancement attributable to pressure wave interaction at the gas-liquid interface is expected to significantly increase the surface area by increasing the rate of droplet formation. Without a droplet formation model, this effect will not be simulated. The CRAFT code contains a Lagrangian solver for tracking droplets, and a pressure-dependent burn rate combustion model could be implemented. Unfortunately, the appropriate rate constants are not available because empirical models of droplet formation are calibrated at much lower pressure and velocity. Therefore, droplet formation was not modeled.

Another consideration is that the operating conditions in the BLPG may be above the critical state of the LP. Accurate values of the critical pressure and temperature of the LP (described in the next section) being used in the experimental studies (Talley & Owczarczak 1994; Rosenberger, Stobie, & Knapton 1995a, 1995b; Talley, Owczarczak, & Geise 1997) are unknown. An estimate of a critical pressure of 250 MPa was made by Faeth, Lee, and Kounalakis (1987); however, the authors attributed an error of as much as 50% to that value. In any case, it is possible that the flow and combustion processes in the BLPG occur above the critical state for a portion of the ballistic cycle. In view of the uncertainties, the gas-liquid formulation was chosen to model the experimental data. This is consistent with the previous BLPG and LPETC modeling efforts.

3. Experimental Fixture

The approach of this study was to perform 2-D axisymmetric simulations of two 30-mm BLPG firings performed in accordance with a U.S. Army contract at Veritay Technology, Inc. (Talley, Owczarczak, & Geise 1997). The objective of the BLPG experimental program was to evaluate the effectiveness of combustion chamber geometry in controlling the interior ballistic variability and overall shape of the pressure-time curves. Figures 2 and 3 show two of the "stepped chamber" configurations that were investigated. It was postulated that by properly configuring the diameter and length of each section, the progressivity and stability of combustion in the chamber could be controlled. It was believed that one mechanism for achieving this was by the promotion of turbulence via the addition of steps in the combustion chamber. The experimental results showed that some control of the ballistic process could be achieved with this

concept, as compared to standard, single-diameter chambers. However, the empirical data indicated the potential for a lack of control late in the ballistic cycle, when the Taylor cavity is expected to extend beyond the stepped region in the chamber.

Figure 2 shows the standard four-stage, stepped chamber. The combustion chamber consisted of four sections that "step" in diameter from 1.6 to 2.0, 2.4, and 2.8 cm, respectively. The gun barrel section, which becomes part of the chamber wall after the projectile moves, was 3.0 cm in diameter. The location of the pressure gauge ports, P1, P2, and P5, is also shown in Figure 2. The combustion chamber was initially completely filled with LP and was 14.2 cm long. The mass of the LP was 85.0 g and the mass of the projectile was 394 g. The process was initiated by the ignition of a small solid propellant charge loaded in the "igniter chamber" (see Figure 2). The igniter charge burned at high pressure and injected hot gas into the combustion chamber, initiating the LP combustion. The size of the igniter chamber orifice was 1.32 mm.

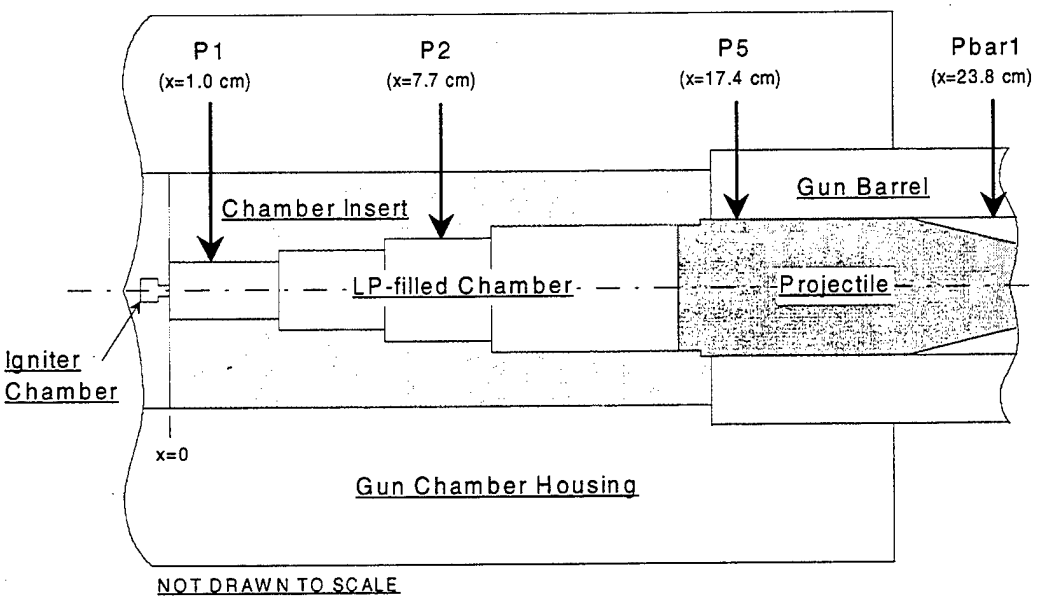

Figure 2. Standard Four-stage Combustion Chamber.

Figure 3 shows a modified version of the four-stage combustion chamber. The diameter of the fourth stage of the chamber was increased to 3.8 cm and then was tapered to 2.8 cm with a 12° taper. The mass of the LP was 114 g and the mass of the projectile was 357 g. The purpose of this design was to increase the ballistic performance (i.e., projectile muzzle velocity) by increasing the LP charge without adversely affecting the stability of the pressure-time curve. Past experience showed that increasing the LP charge by simply increasing the length of the chamber could lead to unrepeatable pressure-time traces. These unrepeatable results usually showed two pressure peaks, with the second peak

likely attributable to the portion of the LP charge that travels with the projectile and burns in the gun barrel, late in the ballistic cycle. If this characteristic were repeatable, it could provide a performance enhancement because of the higher pressure near the projectile. However, this effect was not repeatable and usually led to undesirable variability in muzzle velocity.

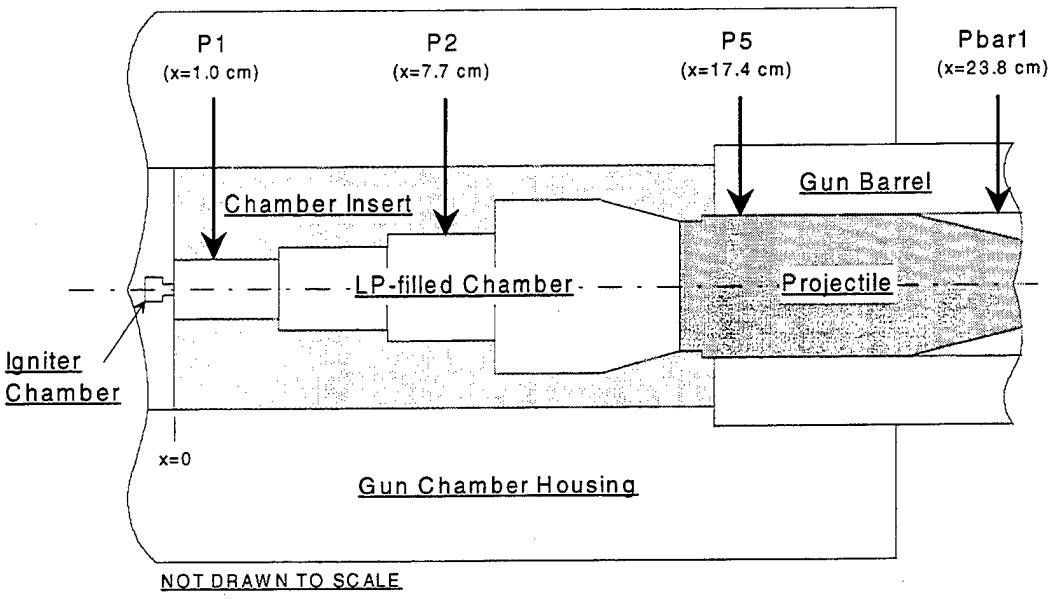

Figure 3. Modified Four-stage Combustion Chamber.

The propellant used in the gun firings was the monopropellant XM46 (formerly designated LGP 1846). The weight-percent composition of XM46 is 19.2% hydroxylammonium nitrate, 60.8% triethanolammonium nitrate, and 20.0% water. The basic thermodynamic properties of XM46 (at 0.2 g/cm^3 loading density) are a flame temperature of 2469 K, an impetus of 898.3 J/g, a molecular weight (product gas) of 22.848, and a frozen specific heat ration (γ) of 1.2225 (Freedman 1988).

4. Results and Discussion

4.1 Simulation Procedure

Two simulations were performed with the chamber configurations shown in Figures 2 and 3. The grids for these two chamber configurations are shown in Figure 4. The simulation was performed as 2-D axisymmetrical, as shown in Figure 4. The lower boundary represents the axis of the combustion chamber. To form the stepped region of the chamber, a grid-blanking procedure was used to remove sections of the grid from the computations. The initial grid sizes were

47 by 66 and 47 by 67, respectively. The right boundary represented the rear face of the projectile and was modeled as a solid, moving boundary. As the projectile moved, a grid-embedding procedure was used to add cells to the computational domain. A cell was added at the last location in the axial direction if the length of the cell became greater than 3.14 mm. Grid embedding was stopped after propellant "burn-out." The last section of the domain (starting 9.3 cm in Figure 4a and at 13.9 cm in Figure 4b) was then allowed to expand for the remainder of the computation, i.e., during the gas expansion process. The maximum number of nodes in the axial direction at the completion of grid embedding was 144 in the configuration of Figure 4a and 157 in the configuration of Figure 4b.

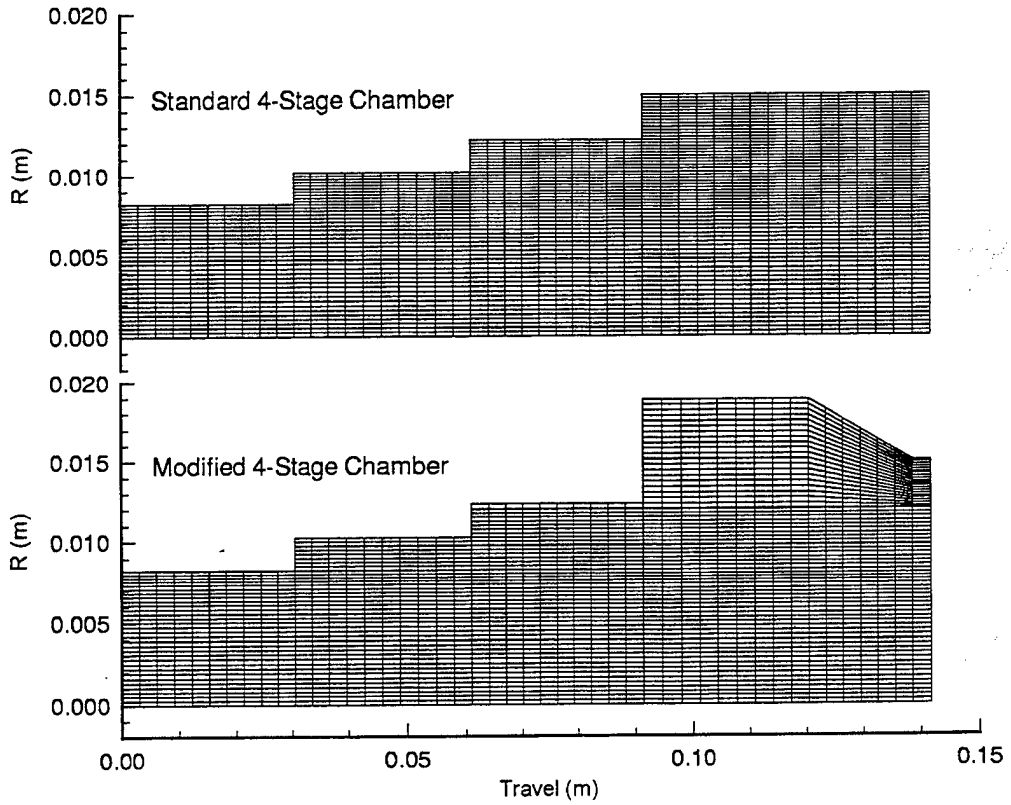

Figure 4. Initial Grids Used in Simulations of the (a) Standard and the (b) Modified Four-stage Combustion Chambers (units are in meters).

The movement of the right boundary, which represented the rear face of the projectile, was based on the equations of motion of a given projectile mass. The acceleration of the projectile was first calculated from the pressure and area at the right boundary and the projectile mass. The velocity and displacement of the right boundary were then calculated. The only loss included in the projectile equation of motion was the frictional force attributable to contact with the gun barrel. A simple resistive force profile was used, with an estimated projectile shot-start pressure of 30 MPa maintained for the first 0.5 cm of travel, decreasing

linearly to 5 MPa at 1.0 cm of travel and remaining at 5 MPa for the remainder of travel. The total projectile travel was 201.7 cm.

The solid boundaries were treated as Euler reflecting boundaries, rather than viscous, no-slip walls. The latter condition would require a large degree of mesh refinement near the walls, including the steps, and was considered too computationally expensive for this study. This limitation was deemed acceptable, even though this boundary condition would have an effect on the near-wall turbulence. The effect on the solution would likely be most pronounced in the stepped region.

Four species were used in the simulation: igniter gas, LP combustion products, LP vapor, and LP liquid. The chamber was initialized as all liquid propellant with the gas volume fraction parameter, ϕ. The igniter gas was only injected during the early part of the simulation and it was included in the combustion products in the plots of combustion product mass fraction. A value of $\phi = 0.02$ was used for the liquid in the combustion chamber, and a value of $\phi_g = 0.99999$ was used for the incoming igniter gases.

The injection of hot combustion gases from the igniter chamber (see Figure 2) was simulated via experimental igniter chamber pressure-time data. This "in-flow" boundary condition was centered at the left end of the axis of the chamber and consisted of the first five cells in the radial direction. The static pressure (from the experimental data), temperature, and velocity vector direction cosines were specified at this in-flow boundary. The in-flow velocity was calculated as part of the solution, with an allowance for choked flow. The properties of the igniter gas in the simulations were the same as LP combustion products, although in the experiments, a solid propellant was used. This was done for convenience only, since the igniter gas represents only a small percentage of the total energy. The temperature of the injected igniter gas was specified as 2000 K.

The initial pressure and temperature in the chamber were set to 1 MPa and 300 K, respectively. Although the initial pressure in the experiment was atmospheric (0.1 MPa), the initial pressure in the simulation was set higher to alleviate a numerical issue in the liquid equation of state calculation. Specifically, a very low pressure would lead to very little change in density and would cause a large round-off error in the iterative routine used to equate the liquid pressure to the gas pressure (equilibrium formulation). The chemical reactions (vaporization and decomposition) were not allowed to begin until the local temperature exceeded 400 K. In addition, a high temperature limit was put on the reaction rate coefficients. The reaction rates at temperatures above 700 K were set to those at 700 K. Without this limitation, the combustion rate was found to increase too much as the temperature increased.

After the simulation began with a value 0.1, the Courant-Friedrich-Levy (CFL) number was increased to 1.0 over the first 2000 iterations (about 0.080 ms). The solution proceeded with a CFL number of 1.0 until about 1.25 ms. The average time step during this time was about 6×10^{-8} sec. After this time, with LP combustion almost complete, the CFL number was raised to 5.0, grid embedding was stopped, and the solution was continued until the projectile reached the maximum gun barrel travel.

4.2 Simulation of Standard Four-Stage Chamber

This simulation was initialized with the conditions of Veritay Test No. 130. One modification in the simulation was that the fourth stage diameter was made 3.0 cm instead of 2.8 cm. This resulted in an increase in the mass of LP in the simulation from 85 g to 93 g—an increase of about 9%. The increase in diameter from the 2.8-cm chamber to the 3.0-cm gun barrel after the projectile moved would have required modification of the dynamic grid routine. It was decided that this was not necessary for these preliminary runs, and the increase in initial chemical energy would be considered when the simulation was compared to the experiment.

Contours of combustion product mass fraction are shown in Figure 5, where the computational domain has been mirrored for illustration. The solution is presented at four times, showing the evolution of combustion and the development of the Taylor cavity. The top plot, at 0.255 ms, shows the development of the combustion gas bubble shortly before the igniter gases stopped venting. Only about 1.5% of the original LP charge combusted to this point. At 0.535 ms, the development of the Taylor cavity is observed. The tip of the cavity is penetrating the liquid at a velocity faster than the projectile velocity. About 17% of the charge has combusted to this point. At 0.695 ms, about 38% of the charge has combusted and there is no liquid left on the wall of the first two stages of the chamber. The cavity tip reaches the projectile base just before the plot shown at 0.923 ms. About 82% of the charge has combusted at this point. Contour plots of vorticity show eddy structures forming past the steps at 0.535 ms, which are well defined at 0.695 ms. Figure 6 shows a contour plot of vorticity at 0.695 ms. It was not determined whether these were turbulent eddies or just laminar wake eddies. However, these eddies may evolve to turbulence that would not be present in the absence of the steps.

In Figures 7 through 9, the simulated pressure-time history is compared with that of Test No. 130 at the P1, P2, and P5 locations (see Figure 2). The P5 location is open to the chamber pressure after passage of the projectile. The experimental pressure-time curves shown here were filtered with a 10-kHz, low-pass filter. The unfiltered curves contained high frequency oscillations usually associated with LP combustion. In general, the simulated maximum mean pressure is higher and occurs later in time than in the experiment. The overall wider shape of the simulated pressure-time curve near peak pressure indicates that

combustion is likely progressing in a more stable manner than in the experiment. In the simulation, the gas cavity reaches the projectile at about 0.9 ms, which is the point at which the pressure begins to decrease (see Figure 8). This is in contrast to the traditional view of the BLPG process, which proposed that combustion enhancement would normally take place at this point. However, the Kelvin-Helmholtz mixing attributed to this process is not included in the simulation.

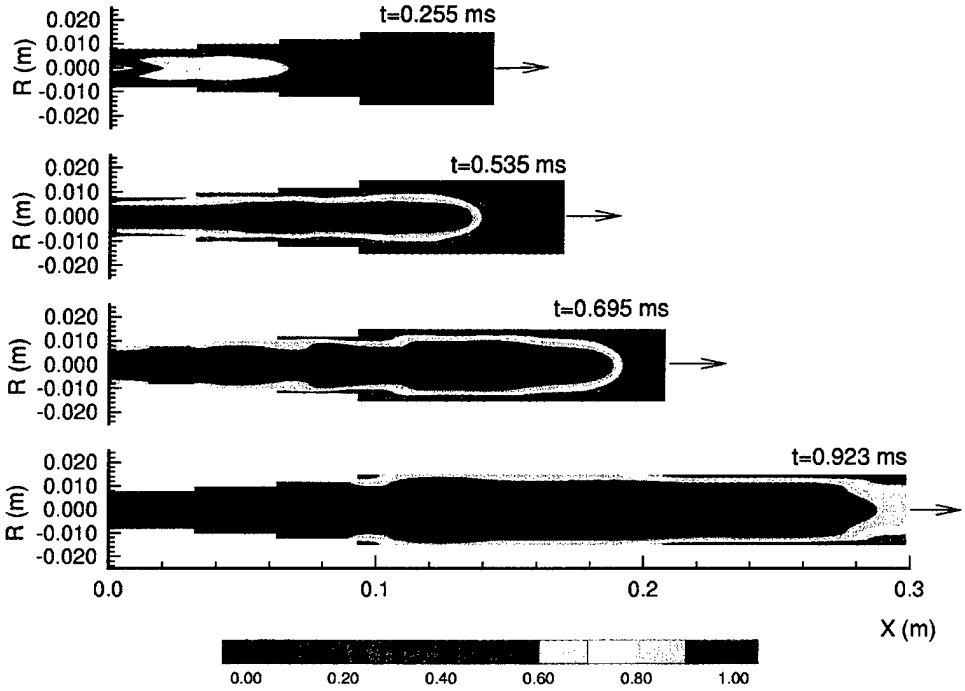

Figure 5. Contours of Combustion Product Mass Fraction for Simulation of Standard Four-stage Chamber at 0.255, 0.535, 0.695, and 0.923 ms.

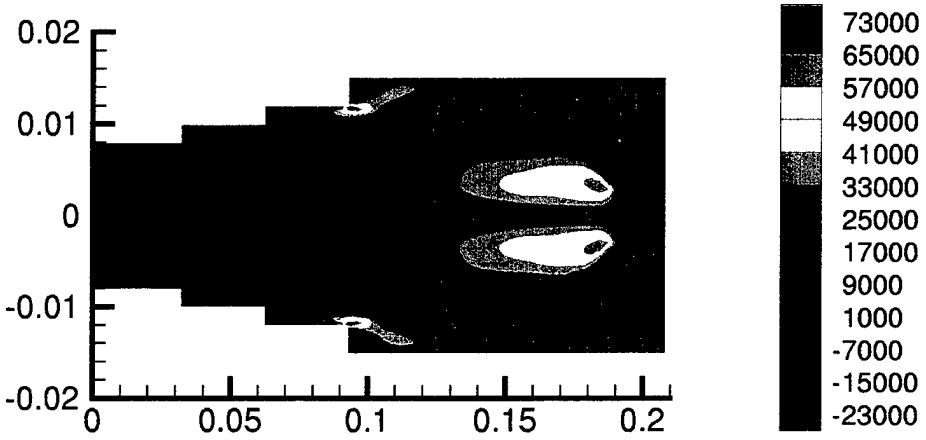

Figure 6. Contours of Vorticity Simulation of Standard Four-stage Chamber at 0.255, 0.535, 0.695, and 0.923 ms.

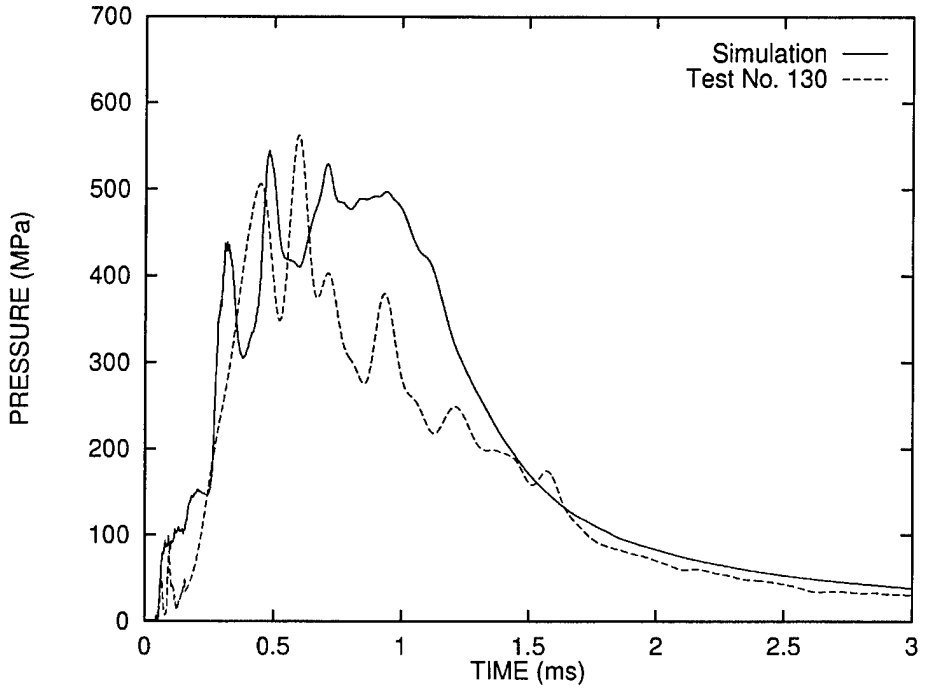

Figure 7. Pressure at P1 Location From Simulation (solid line) and From Test No. 130 (dashed line).

In Figures 7 and 8, it can also be seen that the travel of the blast wave from the igniter orifice (at t = 0.0) to the P1 and P2 locations was captured in the simulation. Also, in the simulation, the pressure, which is driven by the igniter, continues to rise quickly. However, there is a combustion delay of about 0.1 ms in the experiment. During this delay, which is not detrimentally long in this case, there is likely quenching of the igniter gases and a low-energy release, "fizz-burn" of the LP. In the past, longer combustion delays have led to extremely high, undesirable pressures. As set up, the simulation will not capture this combustion delay. Figure 9 shows that the simulation captures the passage of the projectile by the P5 location at the proper time.

The simulation does capture the predominantly longitudinal wave structure that was observed in the experiment. This wave structure is attributable to the pressure pulse caused by the igniter. Examination of contour plots of pressure showed some radial structure early, during the early growth of the gas cavity, but this quickly developed into the longitudinal structure. The longitudinal wave structure is expected with ignition that occurs at the end of the chamber. The frequency of the longitudinal wave structure was a little lower in the simulation. The period between the first two peaks (at about 0.5 ms) was 0.164 ms in the simulation versus 0.149 ms in the experimental case.

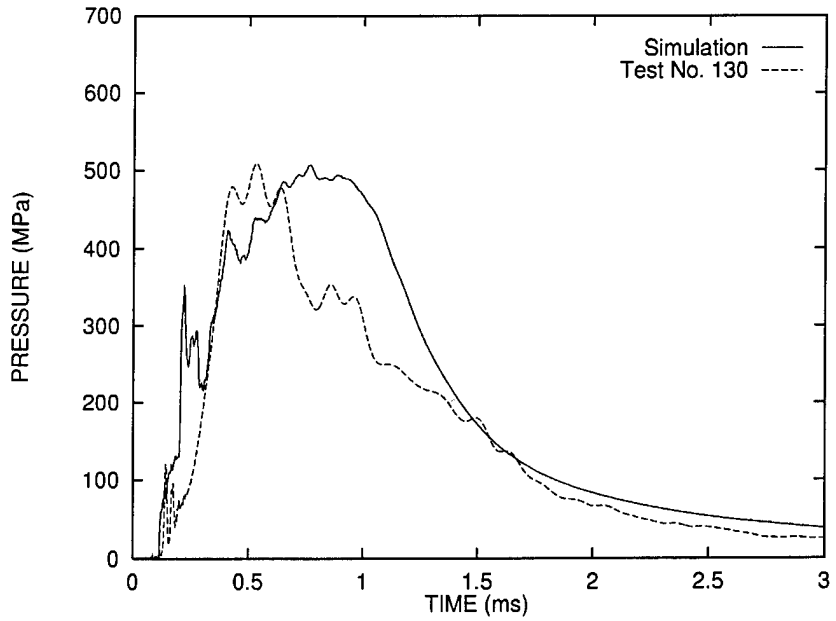

Figure 8. Pressure at P2 Location From Simulation (solid line) and From Test No. 130 (dashed line).

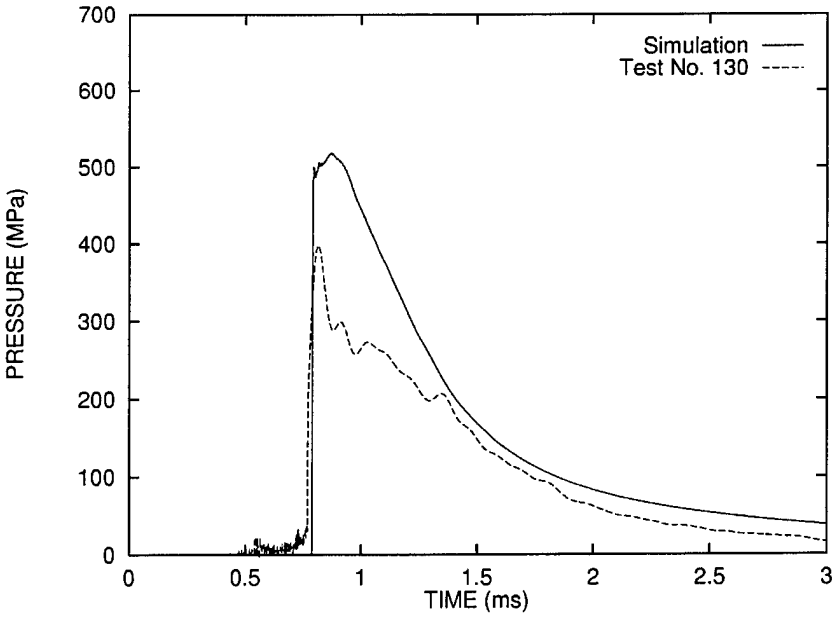

Figure 9. Pressure at P5 Location From Simulation (solid line) and From Test No. 130 (dashed line).

The projectile muzzle velocity in the simulation was 967 m/s, which is much higher (26%) than that measured in the experiment (769 m/s). The 9% increase in chemical energy in the simulation would only account for a small part of this difference because of the ballistic efficiency (projectile muzzle kinetic energy

divided by total chemical energy), which was 34% in Experiment No. 130. No heat transfer losses to the gun tube wall were considered in the calculation, although this would still only account for part of the difference. The velocity difference is attributable to the difference in the pressure-time history of the simulation, as compared to the experimental data. It is obvious that not all the physics of the combustion process are correctly modeled in this case.

4.3 Simulation of Modified Four-Stage Chamber

This simulation was set up with the conditions of Veritay Test No. 155. The rear of the projectile in this experiment was made of plastic and was hemispherical in shape; this was a design modification that alleviated but did not eliminate the adverse effects of the longitudinal wave problem (Talley, Owczarczak, & Geise 1997). The hemispherical base was not modeled for this simulation. However, the length of the flat base design was adjusted so that the difference in volume was only 0.42 cm^3 (1%).

Contours of combustion product mass fraction are shown at four times in Figure 10. When compared to the previous simulation, the gas cavity is observed to reach the chamber wall in the third stage earlier. This is a result of the increased compressibility of the liquid column because of the increased volume in the fourth stage. This also results in a slower penetration of the cavity tip.

The simulated pressure-time history is compared to that of Test No. 155 in Figures 11 and 12. The very large amplitude of the pressure waves in the experimental pressure-time curve in Figure 11 is likely an artifact attributable to amplification in the pressure gauge port cavity (Rosenberger 1994). The projectile muzzle velocity in the simulation was 1086 m/s versus 983 m/s in Test No. 155—a difference of 10%. This simulation compares better with the experimental data than the previous simulation. Comparing the two simulation results, shown in Figure 13, it is observed that the main differences are a shift of the peak pressure to a later time and a slightly higher pressure during the expansion part of the process. The better match with the data in the second simulation is more attributable to the difference in the experimental pressure-time curve, which is wider than in the previous experiment. One may consider that in the second case, Test No. 155, the combustion may have proceeded in a more stable manner, without the anomalous features not modeled in the simulation.

4.4 Discussion of Results

Figure 14 shows contour plots of temperature for the two simulations at about 0.7 ms. The difference in cavity penetration between the two simulations can be observed. It was also observed that the maximum temperature in the gas cavity was about 3200 K, even though the flame temperature is 2469 K (at a loading density of 0.2 g/cm^3). Adjusting for the higher loading density in the BLPG only

density of 0.2 g/cm^3). Adjusting for the higher loading density in the BLPG only increases the flame temperature to about 2600 K. Temperatures higher than the flame temperature in interior ballistic calculations would normally indicate an error in the solution. One possible explanation is the use of a constant specific heat value. Although the CRAFT code allows for a variable specific heat, a constant value was used. The unique conditions in which the BLPG operates led to a search for a possible physical mechanism. The highest temperature is near the core of the gas cavity, not far behind the tip. The temperature in the combustion zone (gas-liquid interface) is at the flame temperature. One might expect the combustion zone to give the highest temperature if numerical error were the problem.

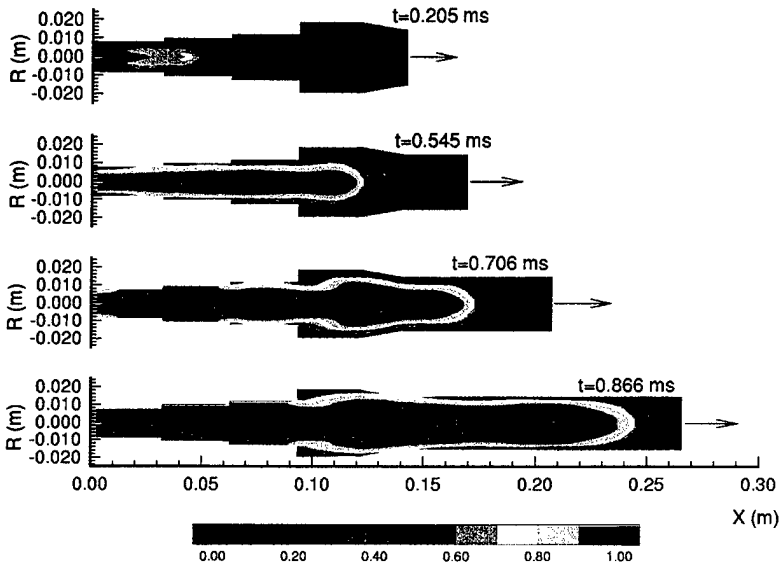

Figure 10. Contours of Combustion Product Mass Fraction for Simulation of Modified Four-stage Chamber at 0.205, 0.545, 0.706, and 0.866 ms.

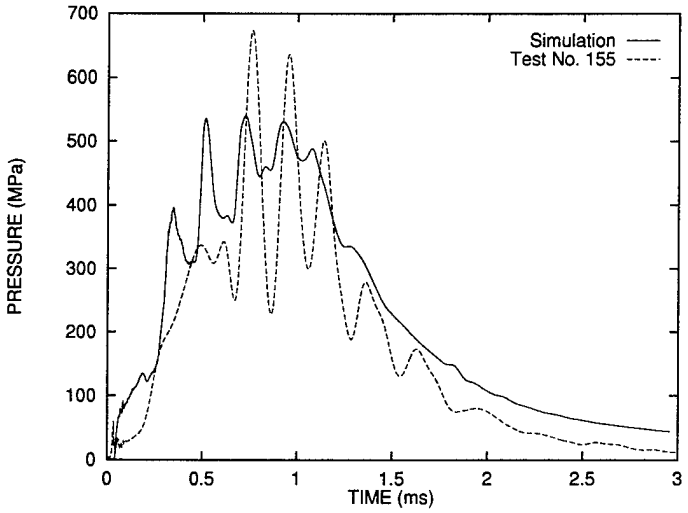

Figure 11. Pressure at P1 Location From Simulation (solid line) and From Test No. 155 (dashed line).

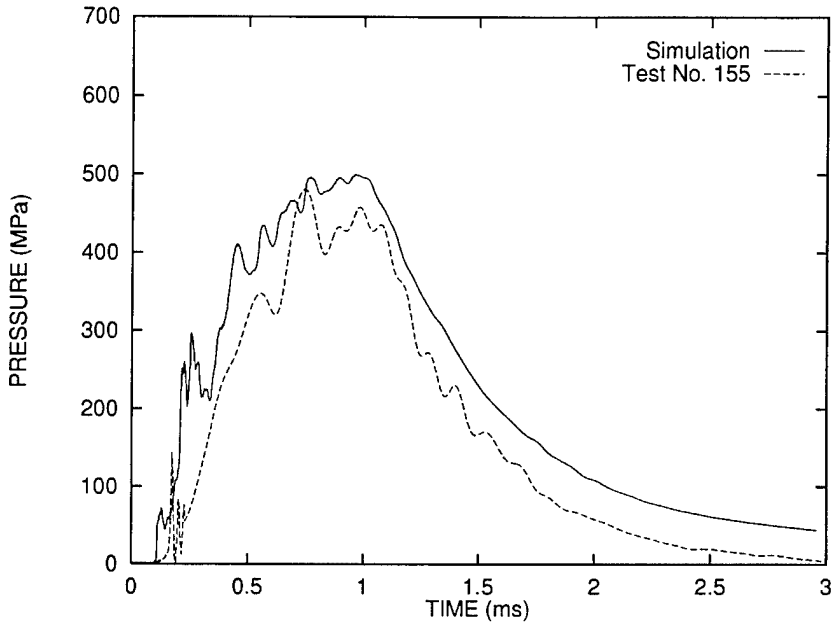

Figure 12. Pressure at P2 Location From Simulation (solid line) and From Test No. 155 (dashed line).

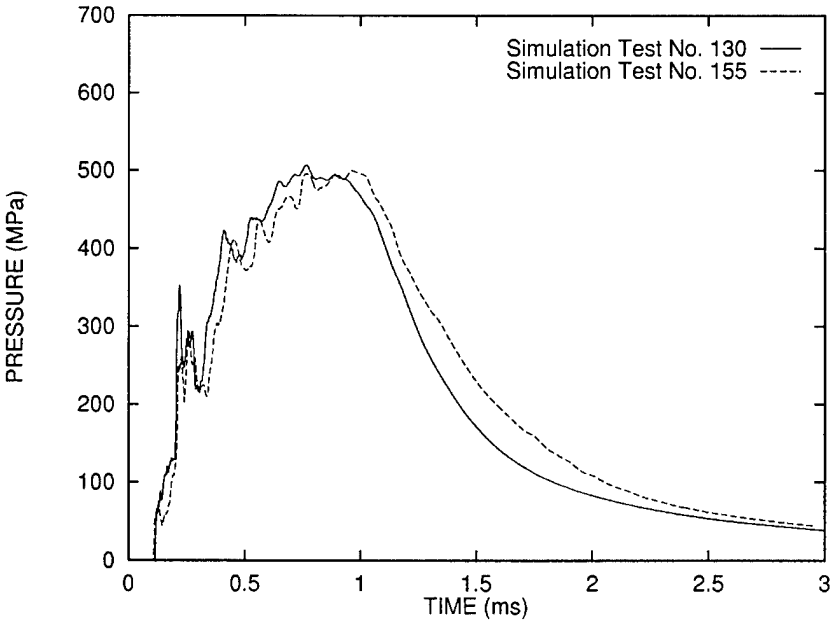

Figure 13. Pressure at P2 Location From Simulation of Test No. 130 (solid line) and From Simulation of Test No. 155 (dashed line).

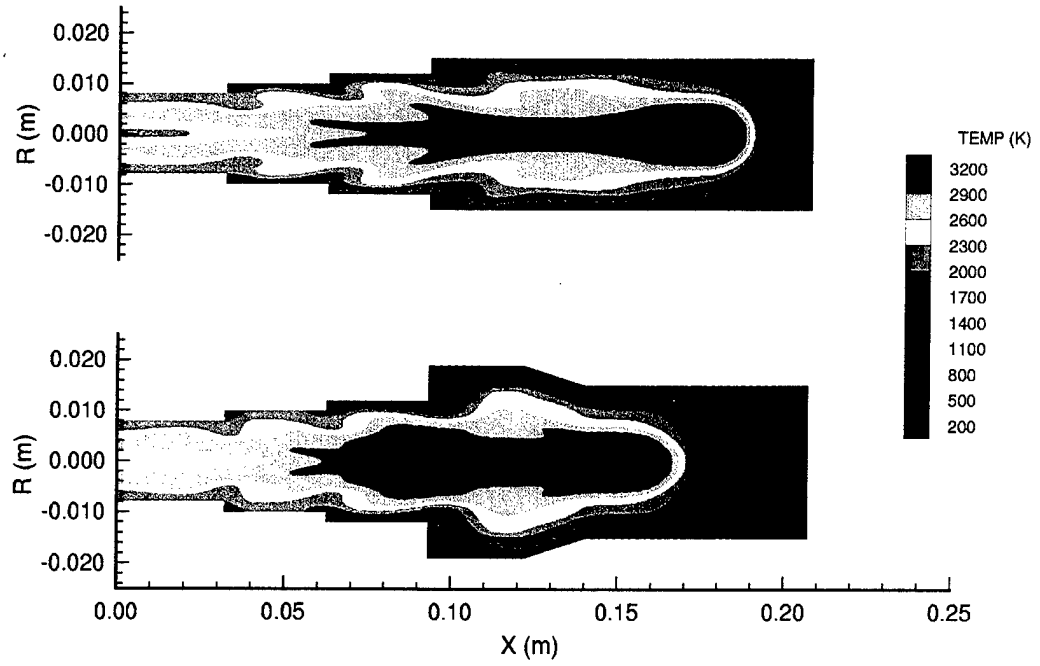

Figure 14. Contours of Temperature (K) for Simulation of Standard (top) and Modified (bottom) Four-stage Chamber.

One possible explanation may be simply isentropic compression of the combustion gases during the ballistic cycle. The process begins when the igniter vents hot gas into an almost incompressible liquid. Relief will be achieved by movement of the projectile and the conversion of LP to gas combustion product. The projectile does not begin to move until about 0.2 ms and the pressure at the P1 location is already about 150 MPa by this time (see Figure 7). Therefore, compression of the igniter vent gases would occur very early. In combustion of solid propellant grains or LP droplets, only the local temperature near the combustion surface will be at the flame temperature. The temperature quickly drops as the combustion gases expand away from the combustion zone. The configuration of the BLPG is such that the combustion gas is surrounded by the combustion zone, which is at or near the flame temperature. In this case, it may be possible for the combustion gases to be compressed above the flame temperature.

In order to check the plausibility of this hypothesis, the simulation of the standard four-stage chamber (Veritay Test No. 130) was examined in more detail. The value of the temperature and pressure in the region behind the cavity tip was extracted from the solution field at about 0.1-ms intervals. If isentropic compression were occurring during this time, assuming a perfect gas model, the relation $Tp^{-(\gamma-1)/\gamma}$ should be constant. In this relation, T is the gas temperature, p is the gas pressure, and γ is the ratio of specific heats. From about 0.3 ms to 0.9 ms, the period of highest temperature, the value of $Tp^{-(\gamma-1)/\gamma}$ varied only about 3.6%, with a γ value of 1.2226. Mass was being added to the system from the igniter

venting process before 0.3 ms. After 0.9 ms, the value of $Tp^{-(\gamma-1)/\gamma}$ decreased about 9%, which coincided with a decrease in total mass of about 1.5%. This mass error occurred during the period of high projectile acceleration. It was likely attributable to both numerical error from the extrapolation used during the grid embedding process and the high CFL number used during this period.

This result indicates that gas compression is a possible explanation for the high gas cavity temperature. This phenomenon was apparently not encountered in previous BLPG modeling. It would not likely be noticed in LPETC gun modeling since the plasma is injected at temperatures above 15,000 K. Future studies should consider this phenomenon, both for added confirmation that it is physical and because of its potential effect on the combustion process.

The results of the two simulations illustrate both the strengths and weaknesses in modeling the BLPG process. Solutions that compare favorably with experimental data can be made, such as in the second simulation. At the same time, other solutions, such as in the first simulation, demonstrate that some physical processes are not being modeled. To further illustrate this limitation, a third simulation was performed. This simulation was set up with the same LP charge volume and projectile mass as the modified four-step chamber simulation, 114 g and 357 g, respectively. However, in this case, a simple cylindrical chamber was considered, similar to the traditional BLPG chamber that was considered in earlier studies. The diameter of the chamber was 3.0 cm and the initial length was 11.3 cm, with an initial grid of 38 by 66. From the experimental point of view, this case would not be expected to have a pressure-time history similar to that of Test No. 155 (see Figures 11 and 12), at least not without proper tuning of the igniter. The pressure-time history was shown experimentally to be sensitive to the igniter orifice/chamber diameter ratio (Talley & Owczarczak 1991, 1994), which was the original basis for using the stepped chamber geometry. The resulting simulation did not show any grossly different features than the previous two simulations, thus indicating insensitivity to geometry, which does not follow the experimental observations. Figure 15 shows a comparison of the simulated pressure at the P1 location from this simulation and the modified four-stage chamber simulation (see Figure 11). The comparison illustrates some physically viable differences in the cylindrical chamber case, such as the lack of amplification of the longitudinal wave structure (discussed in the next paragraph); the slower initial rise rate because of the added compressibility of the increased volume of LP outside the igniter orifice; and the low-amplitude, high-frequency, radial wave structure. The combustion model used in the simulation does not provide the capability to simulate the physical instability mechanisms that appear in the experimental fixture.

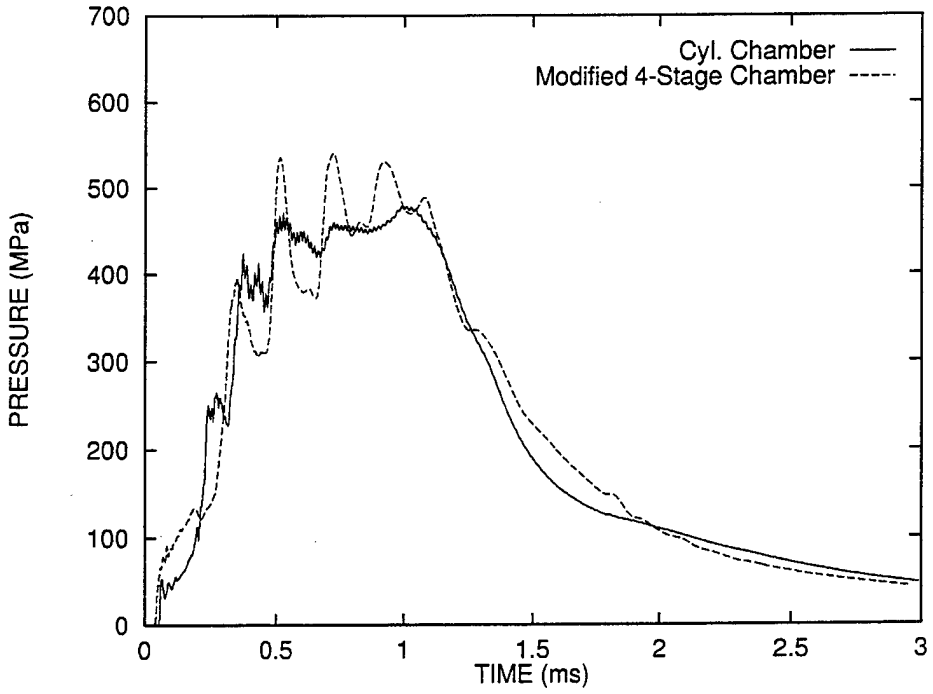

Figure 15. Comparison of Pressure at P1 Location From Simulation Using Cylindrical Chamber Geometry (solid line) and From Simulation Using Modified Four-stage Chamber Geometry (dashed line).

The limitations of the current model reduce its usefulness as a predictive tool. However, it may be useful in helping to analyze experimental data and even give insight for chamber design. For example, in many of the experimental data, high amplitude pressure waves were observed at the P1 location but at a much lower amplitude at the P2 location. It was interesting to see the same phenomenon present in the simulation. The phenomenon is apparently attributable to the wave interactions with the stepped geometry, amplifying the magnitude in the smaller volume, end section where P1 is measured. Although this may be intuitive from the geometry of the chamber, the pressure measurement technique at the P1 location was susceptible to amplification of the signal (Rosenberger 1994), leading one to question whether the magnitude of the pressure waves was reasonable.

It is possible that other physical phenomena may be simulated through the adjustment of some parameters. For example, the combustion delay early in the ballistic cycle might be reproduced by increasing the temperature at which decomposition from LP vapor to combustion products takes place. This would allow the accumulation of LP vapor, which would not increase the pressure very much and would combust rapidly when the decomposition temperature was exceeded. Although this may increase the likelihood of capturing features of the experimental pressure-time trace and may be helpful in understanding the physical processes, it does not necessarily lead to better predictive capability.

The inclusion of better physical models, such as liquid droplet formation and more detailed chemical kinetics, is probably required before a predictive code can be developed. Unfortunately, this is a difficult task, since the applicability of formulations from other work, such as the spray combustion area, is difficult to validate at very high gun pressures. The evaluation of more detailed physical sub-models will require time-consuming comparisons with a good set of experimental data. The evaluation should also be made with various chamber geometry variations, such as the Veritay data, which include several other chamber concepts not discussed in this report (Talley, Owczarczak, & Geise 1997).

5. Summary

A modified version of the CRAFT Navier-Stokes code was used to perform simulations of firings that employ two different bulk-loaded liquid propellant gun chamber configurations. The resulting pressure-time history at several locations in the chamber and gun tube was compared to experimental data obtained in a separate study.

The simulations showed the development of a Taylor cavity that penetrated the bulk-liquid column as it accelerated toward the projectile. This was very similar to the traditional description of the BLPG interior ballistic process described by Comer, Shearer, and Jones (1963). An annulus of unburned liquid propellant remained along the chamber wall in the last section of the four-stage chamber. Eddy structures formed after the steps in the combustion chamber. The simulations also capture the longitudinal wave structure present in the experimental data.

A comparison of the simulation of the first chamber configuration with experimental data showed that the shape of the pressure-time curve was different and the predicted pressure was higher in the simulation. The earlier pressure peak in the data indicated that the combustion occurred faster than the simulation predicted. A combustion delay present in the experimental data was not present in the simulation. An over-prediction of projectile muzzle velocity of 26% followed from the difference in pressure-time history.

The simulation of the second chamber configuration showed a much better match to the overall shape of the pressure-time curve of the experimental data. The peak pressure in the simulation was still too high and the projectile muzzle velocity was over-predicted by 10%. Since the overall shape of the pressure-time curve in both simulations was similar, the better match with data in the second experimental case was attributed to the processes in the second experiment proceeding in a more stable manner, similar to that modeled in the simulation.

Temperatures higher than the LP flame temperature were observed in the gas cavity region. It was proposed that isentropic compression was a plausible explanation for the phenomenon. Further study of this phenomenon is warranted.

The model does not yet contain sufficient physics present in the BLPG to be a predictive tool but may be useful as a tool to help analyze experimental data. These results confirm that numerical tools are available and are capable of providing solutions to this very complex physical system. However, the emphasis in future work should be on the inclusion of the missing physical models, such as droplet formation and combustion and liquid propellant chemical kinetics.

References

Burnett, W.M., "An Interior Ballistics Model for Liquid Propellant Guns." IHTR 444, Naval Ordnance Station, Indian Head, MD, September 1976.

Chakravarthy, S.R., and S. Osher, "Numerical Experiments with the Osher Upwind Scheme for the Euler Equations." *AIAA Journal*, Vol. 21, No. 9, pp. 1241-1248, September 1983.

Chen, J.L., K.K. Kuo, and F.B. Cheung, "Theoretical Modeling of the Interior Ballistic Processes in an Electrothermal Chemical Gun." *Journal of Propulsion and Power*, Vol. 8, No. 3, pp. 655-666, May-June 1992.

Comer, R.H., R.B. Shearer, and R.N. Jones, "Interior Ballistics of Liquid Propellant Guns." Report No. 1205, U.S. Army Ballistic Research Laboratory, Aberdeen Proving Ground, MD, May 1963.

Cook, D.C., J.A. Dyvik, and G.S. Chryssomallis, "A Multidimensional Electrothermal Model." *Proceedings of the 26th JANNAF Combustion Subcommittee Meeting*, CPIA Publication 529, vol. III, pp. 119-126, October 1989.

DeSpirito, J., Unpublished data, U.S. Army Ballistic Research Laboratory, August 1988.

Edelman, R.B., "The Interior Ballistics of Liquid Propellant Guns." RDA-TR-4400-010, R&D Associates, Santa Monica, CA, August 1974.

Edelman, R.B., "A Transient Quasi-One Dimensional Model of the Interior Ballistics Process for Non-Hypergolic Liquid Bi-Propellant Guns." RDA-TR-8700-001, R&D Associates, Santa Monica, CA, September 1976.

Edelmen, R.B., G.T. Phillips, and T.S. Wang, "Analysis of Interior Ballistics Processes of Bulk-Loaded Liquid Propellant Guns." Final Report 83-048, Science Applications, Inc., Chatsworth, CA, May 1983.

Faeth, G.M., T.W. Lee, and M.E. Kounalakis, "Mixing and Thermodynamic Critical Phenomena of Combusting Monopropellant Sprays." *Proceedings of the 24th JANNAF Combustion Subcommittee Meeting*, CPIA Publication 476, Vol. I, October 1987.

Freedman, E., "Thermodynamic Properties of Military Gun Propellants." In *Gun Propulsion Technology*, edited by L. Stiefel, Vol. 109, Progress in Astronautics and Aeronautics, AIAA, pp. 103-132, Washington, DC, 1988.

Hosangadi, A., N. Sinha, and S.M. Dash, "Multi-Dimensional Simulation of ETC Gun Flowfields." ARL-CR-240, U.S. Army Research Laboratory, Aberdeen Proving Ground, MD, August 1995.

Hosangadi, A., D.C. Kenzakowski, N. Sinha, and S.M. Dash, "Combustion Instabilities in Interior Ballistic Flowfields." AIAA-96-3078, Lake Buena Vista, FL, July 1996.

Hsiao, C.C., G.T. Phillips, and F.Y. Su, "A Numerical Model for ETC Gun Interior Ballistics Applications." *Proceedings of the 29th JANNAF Combustion Subcommittee Meeting*, CPIA Publication 593, Vol. I, pp. 367-376, October 1992.

Klingenberg, G., J.D. Knapton, W.F. Morrison, and G.P. Wren, "Liquid Propellant Gun Technology," *Progress in Astronautics and Aeronautics*, AIAA, Washington, DC, 1997.

Kuo, K., F.B. Cheung, and J.L. Chen, "A Multi-Phase Multi-Dimensional Transient Bulk-Loaded Liquid Propellant Gun Model." *Proceedings of the 11th International Symposium on Ballistics*, 1989.

Macpherson, A.K., A.J. Bracuti, and D.S. Chiu, "Modeling of a Bulk Loaded Liquid Propellant Gun." *Proceedings of the 31st JANNAF Combustion Subcommittee Meeting*, CPIA Publication 620, Vol. III, pp. 295-303, October 1994.

Madabhushi, R.K., A. Hosangadi, N. Sinha, and S.M. Dash, "Large Eddy Simulation Studies of Vortex Shedding with Application of LPG Instabilities Using the CRAFT Navier-Stokes Code." ARL-CR-241, U.S. Army Research Laboratory, Aberdeen Proving Ground, MD, August 1995.

Molvik, G.A., and C.L. Merkle, "A Set of Strongly Coupled, Upwind Algorithms for Computing Flows in Chemical Nonequilibrium." AIAA-89-0199, Reno, NV, January 1989.

Morrison, W.F., J.D. Knapton, and M.J. Bulman, "Liquid Propellant Guns." In *Gun Propulsion Technology*, edited by L. Stiefel, Vol. 109, Progress in Astronautics and Aeronautics, AIAA, pp. 413-471, Washington, DC, 1988.

Roe, P.L., "Approximate Reimann Solvers, Parameter Vectors, and Difference Schemes." *Journal of Computational Physics*, Vol. 43, pp. 357-372, 1981.

Rosenberger, T.E. "Workshop Report: Measurement Techniques in Highly Transient, Spectrally Rich Combustion Environments." ARL-SR-18, U.S. Army Research Laboratory, Aberdeen Proving Ground, MD, September 1994.

Rosenberger, T.E., I.C. Stobie, and J.D. Knapton, "Test Results from a 37-mm Segmented-Chamber Bulk-Loaded Liquid Propellant Gun." ARL-TR-871, U.S. Army Research Laboratory, Aberdeen Proving Ground, MD, September 1995a.

Rosenberger, T.E., I.C. Stobie, and J.D. Knapton, "Test Results from a 30-mm Segmented-Chamber Bulk-Loaded Liquid Propellant Gun." *Proceedings of the 32nd JANNAF Combustion Subcommittee Meeting*, CPIA Publication 631, Vol. I, pp. 231-246, October 1995b.

Sinha, N., S.M. Dash, and A. Hosangadi, "Applications of an Implicit, Upwind Navier-Stokes Code, CRAFT, to Steady/Unsteady Reacting, Multi-phase Flowfields." AIAA-92-0837, Reno, NV, January 1992.

Sinha, N., S.M. Dash, and R.K. Madabhushi, "Recent Advances in Jet Flowfield Simulation: Part II - Unsteady Flows." AIAA Paper 93-4391, October 1993.

Talley, R.L., and J.A. Owczarczak, "Ballistic Testing of Liquid Propellant in a Bulk-Loaded Gun with Combustion Control Features." Report No. C90-001, Veritay Technology, Inc., East Amherst, NY, September 1991.

Talley, R.L., and J.A. Owczarczak, "Investigation of Bulk-Loaded Liquid Propellant Gun Concepts." ARL-CR-127, U.S. Army Research Laboratory, Aberdeen Proving Ground, MD, April 1994.

Talley, R.L., J.A. Owczarczak, and M. Geise, "Investigation of Bulk-Loaded Liquid Propellant Gun Concepts." ARL-CR-335, U.S. Army Research Laboratory, Aberdeen Proving Ground, MD, September 1997.

Taylor, G.I., "The Instability of Liquid Surfaces When Accelerated in a Direction Perpendicular to Their Planes, I." *Proceedings of the Royal Society (London), Series A:* 201, 1950.

INTENTIONALLY LEFT BLANK

NO. OF COPIES ORGANIZATION

1 ADMINISTRATOR
DEFENSE TECHNICAL INFO CTR
ATTN DTIC OCA
8725 JOHN J KINGMAN RD
STE 0944
FT BELVOIR VA 22060-6218

1 DIRECTOR
US ARMY RSCH LABORATORY
ATTN AMSRL CI AI R REC MGMT
2800 POWDER MILL RD
ADELPHI MD 20783-1197

1 DIRECTOR
US ARMY RSCH LABORATORY
ATTN AMSRL CI LL TECH LIB
2800 POWDER MILL RD
ADELPHI MD 207830-1197

1 DIRECTOR
US ARMY RSCH LABORATORY
ATTN AMSRL D D SMITH
2800 POWDER MILL RD
ADELPHI MD 20783-1197

1 CDR US ARMY ARDEC
ATTN WECAC WEE D DOWNS
BLDG 3022B
PICATINNY ARSENAL NJ
07806-5000

1 CMDT US ARMY ARMOR CTR
ATTN ATSB CD MLD
FT KNOX KY 40121

1 CMDT USAFAS
ATTN ATST TSM CN
FT SILL OK 78503-5600

1 US MILITARY ACADEMY
MATH SCI CTR EXCELLENCE
ATTN MADN MSCE MAJ HUBER
THAYER HALL
WEST POINT NY 10996-1786

3 CRAFT TECH INC
CMBSTN RSCH AND FLOW TECH
ATTN S DASH N SINHA
A HOSANGADI
174 N MAIN ST BLDG 3
DUBLIN PA 18917

NO. OF COPIES ORGANIZATION

1 VERITAY TECH INC
ATTN E FISHER
4845 MILLERSPORT HWY
PO BOX 305
EAST AMHERST NY 14051-0305

1 PENN STATE UNIV
DEPT OF MECH ENG
ATTN K K KUO
140 RSCH BLDG EAST
UNIVERSITY PK PA 16802

ABERDEEN PROVING GROUND

2 DIRECTOR
US ARMY RSCH LABORATORY
ATTN AMSRL CI LP (TECH LIB)
BLDG 305 APG AA

1 DIRECTOR
US ARMY RSCH LABORATORY
ATTN AMSRL CI N RADHAKRISHNAN
BLDG 394

1 DIRECTOR
US ARMY RSCH LABORATORY
ATTN AMSRL CI H C NIETUBICZ
BLDG 394

2 DIRECTOR
US ARMY RSCH LABORATORY
ATTN AMSRL WM E SCHMIDT
T ROSENBERGER
BLDG 4600

2 DIRECTOR
US ARMY RSCH LABORATORY
ATTN AMSRL WM B A HORST
W CIEPIELLA
BLDG 4600

1 DIRECTOR
US ARMY RSCH LABORATORY
ATTN AMSRL WM BA D LYON
BLDG 4600

NO. OF
COPIES ORGANIZATION

8 DIRECTOR
US ARMY RSCH LABORATORY
ATTN AMSRL WM BC P PLOSTINS
J DESPIRITO (5 CYS)
J SAHU P WEINACHT
BLDG 390

8 DIRECTOR
US ARMY RSCH LABORATORY
ATTN AMSRL WM BE B FORCH
M NUSCA J COLBURN
P CONROY T MINOR
C LEVERITT T COFFEE
A BIRK
BLDG 390

1 DIRECTOR
US ARMY RSCH LABORATORY
ATTN AMSRL WM BF
J LACETERA
BLDG 390

ABSTRACT ONLY

1 DIRECTOR
US ARMY RSCH LABORATORY
ATTN AMSRL CI AP TECH PUB BR
2800 POWDER MILL RD
ADELPHI MD 20783-1197

REPORT DOCUMENTATION PAGE

Form Approved
OMB No. 0704-0188

1. AGENCY USE ONLY *(Leave blank)*	2. REPORT DATE	3. REPORT TYPE AND DATES COVERED
	January 2001	Final

4. TITLE AND SUBTITLE

Interior Ballistic Simulations of the Bulk-Loaded Liquid Propellant Gun

5. FUNDING NUMBERS

PR: 62618AH80

6. AUTHOR(S)

DeSpirito, J. (ARL)

7. PERFORMING ORGANIZATION NAME(S) AND ADDRESS(ES)

U.S. Army Research Laboratory
Weapons & Materials Research Directorate
Aberdeen Proving Ground, MD 21005-5066

8. PERFORMING ORGANIZATION REPORT NUMBER

9. SPONSORING/MONITORING AGENCY NAME(S) AND ADDRESS(ES)

U.S. Army Research Laboratory
Weapons & Materials Research Directorate
Aberdeen Proving Ground, MD 21005-5066

10. SPONSORING/MONITORING AGENCY REPORT NUMBER

ARL-TR-2316

11. SUPPLEMENTARY NOTES

12a. DISTRIBUTION/AVAILABILITY STATEMENT

Approved for public release; distribution is unlimited.

12b. DISTRIBUTION CODE

13. ABSTRACT *(Maximum 200 words)*

The objective of this study was to determine the feasibility of modeling the interior ballistic processes of the bulk-loaded liquid propellant gun. A modified version of the CRAFT Navier-Stokes code was used to perform simulations of bulk-loaded liquid propellant gun firings that employed two different chamber configurations. The simulation accurately captures the longitudinal wave structure present in the experimental data, but a combustion delay present at the start of the ballistic cycle was not present in the simulations. The simulations showed the development of a cavity that penetrated the bulk-liquid column as it accelerated toward the projectile, leaving an annulus of unburned liquid propellant along the chamber wall. High gas temperatures were noted in this gas cavity region, possibly attributable to isentropic compression caused by the unique conditions in the bulk-loaded gun. The simulation of the second chamber configuration compared well with the experimental data, while the simulation of the first chamber configuration did not capture the experimental pressure-time profile. In general, the simulations showed an insensitivity to chamber geometry that is not observed in experimental firings. The limitations of the simulations were attributed to the lack of complete physical sub-models, such as a droplet formation/combustion model and detailed chemical kinetics. The model has the potential to be a useful tool in the analysis of experimental data. However, predictive capability is unlikely without the development of better physical sub-models.

14. SUBJECT TERMS		15. NUMBER OF PAGES
BLPG	interior ballistics	35
computational fluid dynamics	liquid propellant gun	16. PRICE CODE

17. SECURITY CLASSIFICATION OF REPORT	18. SECURITY CLASSIFICATION OF THIS PAGE	19. SECURITY CLASSIFICATION OF ABSTRACT	20. LIMITATION OF ABSTRACT
Unclassified	Unclassified	Unclassified	